

The Sun: The First 4.6 Gyr

Frederick M. Walter¹

Abstract.

I present an overview of some observations of young and active solar-like stars with non-solar-like characteristics. I ask whether the solar analogy can be extrapolated to explain very active stars without violating simple geometrical constraints. Is a young and active star merely an extreme version of today's Sun, with the same atmospheric structures but with filling factors reaching (or exceeding) unity? In light of evidence for large scale quasi-dipolar magnetic topologies on the young and restless stars, maybe it is time to rethink our paradigms.

There is something fascinating about science. One gets such wholesale returns of conjecture out of such a trifling investment of fact.
Mark Twain -- Life on the Mississippi

Despite appearances, this is not a review of the evolution of stellar magnetic activity. It is, rather, a set of variations on a theme: the solar analogy, as a guide to the interpretation of the coronae and chromospheres of the most active stars, needs to be reconsidered. You may alternatively consider this an extended introduction and overview, designed to set the scene for the contributed papers in this session. To that end, making no pretense of being complete or unbiased, I present a series of observations focussed on non-solar-like properties in active cool stars, intended to provoke discussion.

Our paradigm has long been that stellar magnetic activity is just like solar magnetic activity, only ever-so-much-more-so. Observationally, magnetic activity is related to the stellar rotation rate (Simon 2001). Zeeman measurements show that late-type stars with measurable magnetic fields seem to have maximum magnetic field strengths in the range 1-3 kG. Saar (2001) has shown that the product fB scales with activity levels, $fB = 60 Ro^{-1.2}$, where Ro is the Rossby number. The clear inference is that all it takes to make an active star out of the Sun is to give it a magnetic filling factor approaching unity. But this raises uncomfortable questions. What do we mean by the stellar photosphere when the filling factor for starspots approaches or exceeds 50%? How do you increase the solar activity a thousandfold when the active region filling factor reaches a few tens of percent at solar maximum (Orlando et al 2001), and the filling factor of the corona, as estimated from high resolution images, is substantial (see Fig 1)? Perhaps high densities and higher temperatures can save the day. But as we shall see, there is evidence for another kind of magnetic structure

¹Stony Brook University

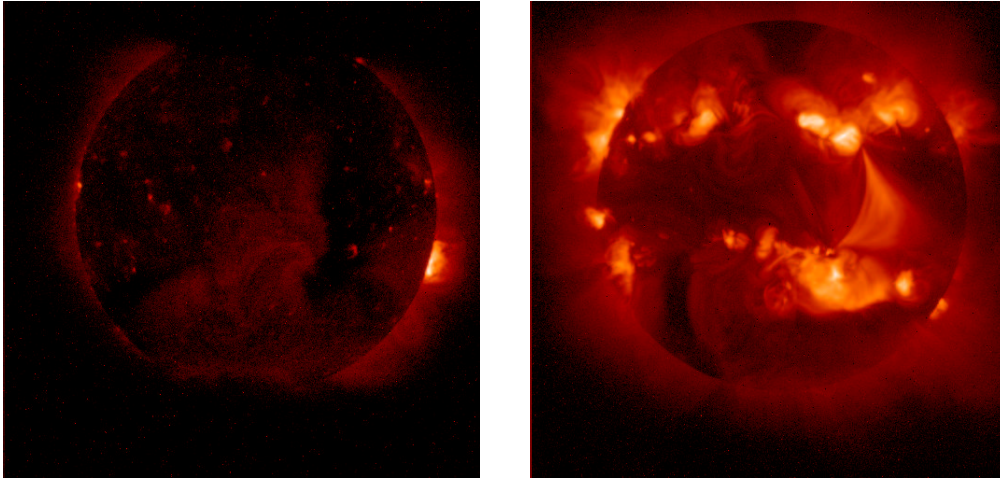


Figure 1. **Left:** A YOHKOH SXT image of the Sun (0.25-4 keV) in a relatively quiet phase of the solar cycle, on 24 May 1995. **Right:** Another aspect of the Sun: A YOHKOH image of a fairly active Sun, on 16 February 1999.

on the young and active stars that is no longer obvious in our Sun. Perhaps we should not try to shoehorn too much into the solar paradigm.

Our direct knowledge of the history of solar activity extends back a few hundred years, and proxy indicators (e.g., $\frac{O^{18}}{O^{16}}$ in ice cores) can extend that back a few tens of thousands of years, less than 1 part in a million of the solar lifetime. We can infer, from the presence of life on Earth, that the Sun wasn't searing the Earth with lethal flares¹ by about 3.8 Gya (10^9 years ago), at an age of about 600 Myr (million years). Table 1 gives an overview of some basic solar parameters at four major junctures in the history of the Solar System: shortly after it crossed its birthline; the time of the last major impact, which led to the formation of the Earth-Moon system; the first evidence of life on Earth; and today. Note that 600 Myr is roughly the age of the Hyades, considered a relatively old cluster. Stellar activity is the domain of the young.

It is traditional to start with our Sun and work backwards through time, slowly spinning the Sun up and increasing the magnetic flux and the filling factor of active regions, while maintaining a star that looks more-or-less like today's Sun, except in degree. I submit that this is not the best way to learn how the early Sun behaved. Rather, it may make sense to start at the beginning. The youngest convective stars do not look like the Sun, yet they will evolve over time into a star like the Sun.

So, how do we get there from here?

¹Since early life was found in the oceans, and not on land, this is not a particularly strong constraint. The atmosphere and the upper few meters of the ocean provide a lot of protection against ionizing radiation.

Table 1. The Sun: Now and Then

Event:	Today	Life appears	Last major impact	PMS Star	
age	4500	600	100	2	Myr
L_{opt}^a	4×10^{33}	3.6×10^{33}	3×10^{33}	3.7×10^{33}	erg s^{-1}
L_X^b	10^{27-28}	10^{29}	10^{30}	10^{31}	erg s^{-1}
T_{eff}^c	5780	5740	5300	3800	K
f_{ion}^d	1	100	1000	10^4	

^a L_{opt} : photospheric luminosity.

^b L_X : coronal X-ray luminosity, a measure of the magnetic activity.

^c T_{eff} : photospheric temperature.

^d f_{ion} : ionizing flux, relative to today. See Walter & Barry (1991).

1. Part I. The Pre-Main Sequence Sun: The Young and the Restless

The young Sun bore only a faint resemblance to today's stable main sequence star. At an age of about 2 Myr (about the present age of the Taurus T association, or of the Orion OB1b association), the young Sun has a radius $R \sim 2R_{\odot}$, a photospheric temperature $T_{eff} \sim 3800\text{K}$, and a bolometric luminosity about 9% less than today's Sun, based on the Baraffe et al (1998) evolutionary tracks. Stellar magnetic activity is almost ubiquitous among the low mass PMS stars: Feigelson (this volume) summarizes the X-ray properties of the 1100 (slightly younger) PMS stars in the Orion Nebula Cluster.

A recent compilation of reviews about low mass pre-main sequence (PMS) stars and their evolution is in *Protostars and Planets IV*, eds. V. Mannings, A.P. Boss, & S.S Russell, (University of Arizona Press, 2000), but there is no review that specifically addresses the properties of the stars themselves. Hartmann (2001) reviewed PMS evolution in the previous Cool Stars Workshop. A not too out-of-date review of the properties of low mass pre-main sequence stars is that of Bertout (1989). Feigelson & Montmerle (1999) reviewed magnetic activity in PMS stars.

1.1. Properties of PMS stars

The low mass pre-main sequence stars are conveniently divided into three classes (Adams et al 1987; Lada 1991) based on their overall spectral energy distributions (SED). Class III sources have approximately blackbody SEDs (i.e., normal stellar photospheres). Class II sources exhibit three spectral components: the stellar photosphere dominating at optical wavelengths, a near-UV excess, and a broad IR excess with a negative spectral index longward of $2.2\mu\text{m}$ attributable to a circumstellar disk. In Class I sources the emission is dominated by a broad SED peaking in the IR, with positive spectral index longward of $2.2\mu\text{m}$. The stellar photosphere is nearly completely veiled by the continuum emission. More recently, Class 0 (André et al 1993) was defined to account for the heavily embedded accreting protostars. The classes form an evolutionary sequence as the circumstellar material fades and the stellar photosphere becomes dominant.

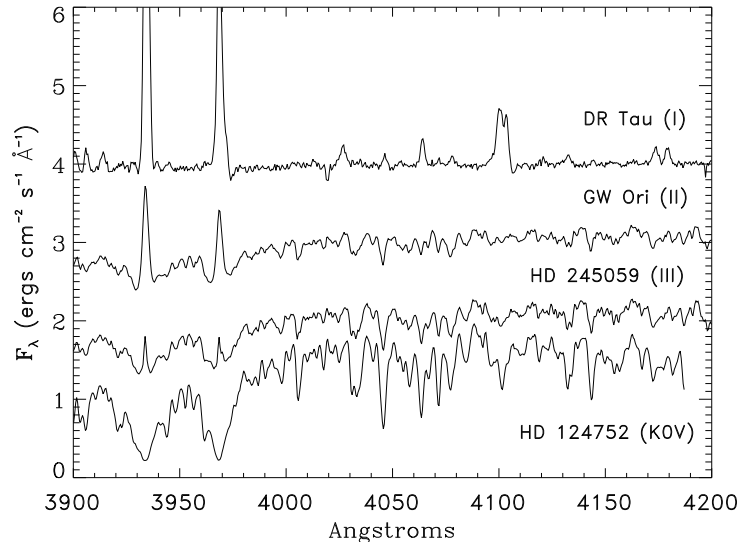


Figure 2. A comparison of early K spectral type PMS stars in the blue region of the optical spectrum. The median continuum levels are normalized to unity, and stars are offset from each other by one unit. Due to blue veiling, DR Tau (Class I) shows no photospheric absorption, although inverse P Cygni profiles indicative of mass infall are seen on the red wings of $H\delta$ and $H\epsilon$ (blended with the Ca II H line). GW Ori, a Class II star, has some veiling, filled-in Balmer lines, and strong Ca II H & K reversals. The Class III star HD 245059 shows an active chromosphere, but no evidence for mass accretion or of a circumstellar disk. At this resolution, the chromospheric H & K reversals are not visible in the spectrum of the old (250 Myr; UMa cluster) K0V star HD 124752.

Sample optical spectra of Class I, II, and III stars are shown in Figures 2 and 3.

Class 0 Even the very youngest protostars, the Class 0 stars, seem to have at least sporadic magnetic activity. These stars are actively accreting, with both circumstellar disks and spherically infalling. The evidence for magnetic activity comes primarily from the observations of hard X-ray flares from embedded protostars (e.g., Montmerle et al 2000). Tsuboi et al (2000) interpreted the hard-X ray light curve seen with ASCA from the protostar YLW 15 as a sequence of flares. Their isothermal solar loop model fits to the exponentially decaying flux, temperature, and emission measure suggest loop lengths of up to 14 stellar radii (loop heights of 4.5 stellar radii if circular).

Class I The Continuum Stars are actively accreting from the circumstellar medium. The accretion luminosity is comparable to or exceeds the photospheric luminosity in the optical. The name is a consequence of the featureless optical spectrum (with emission lines) seen at low dispersion. The veiling (dilution

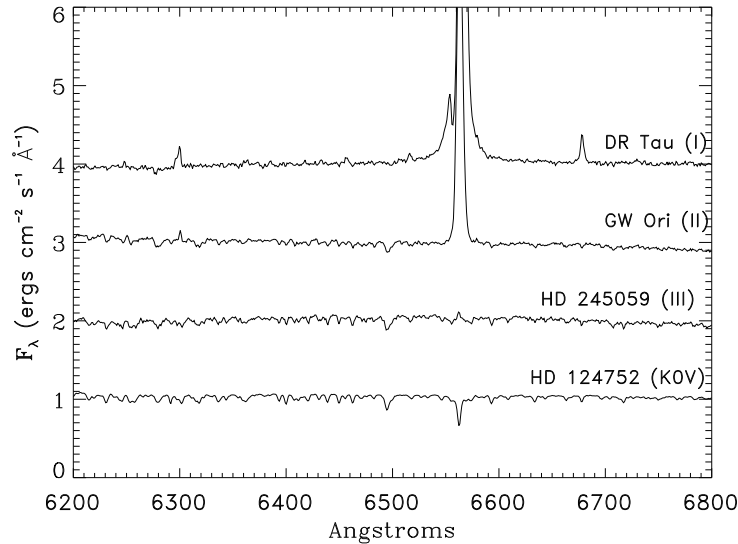


Figure 3. Spectra of the stars shown in Figure 2 in the red region of the optical spectrum. Note the broad $H\alpha$ emission and P Cygni absorption, indicative of a stellar wind, in DR Tau. The chromospheric emission fills in the $H\alpha$ line in HD 245059. $\text{Li I } \lambda 6707\text{\AA}$ is present, but hard to see at this scale.

of the absorption lines by excess continuum; see Hartigan et al 1989) is large. There may be optically-thin spherical infall in some cases. Weak X-ray emission and strong flares are seen in some Class I sources. Examples of Class I objects include L1555 IRS5, RU Lupi, DR Tau, RW Aur, S CrA, and AS 353.

The emission lines in the Class I and II objects arise from 3 sources (Figure 4):

- Strong low excitation lines (O I, Mg II, $H\alpha$) from the stellar wind, and from high up in the accretion stream (Ardila et al 2002b).
- Narrow H_2 Lyman lines from the circumstellar environment, fluorescently pumped by H I Lyman α (Ardila et al 2002a).
- Strong, broad hot lines (C IV, Si IV) arising near the accretion shock. In stars like RU Lupi and T Tauri, the luminosity in these high temperature lines exceeds about $10^{31} \text{ erg s}^{-1}$.

Class II The Classical T Tauri Stars are actively accreting and magnetically active. All are highly variable. Many have long-lived dark spots (e.g., Herbst et al 1982). Some have light curves which suggest bright rather than dark surface spots (e.g., Simon et al 1990). Many Class II stars have winds (see Gomez de Castro, this volume). Examples of actively accreting Class II objects include T Tau N, BP Tau, RY Tau, and TW Hya (Alencar, this volume).

Not all Class II objects are classical T Tauri stars. A subset of the Class II objects have passive disks - disks that intercept and reradiate photospheric

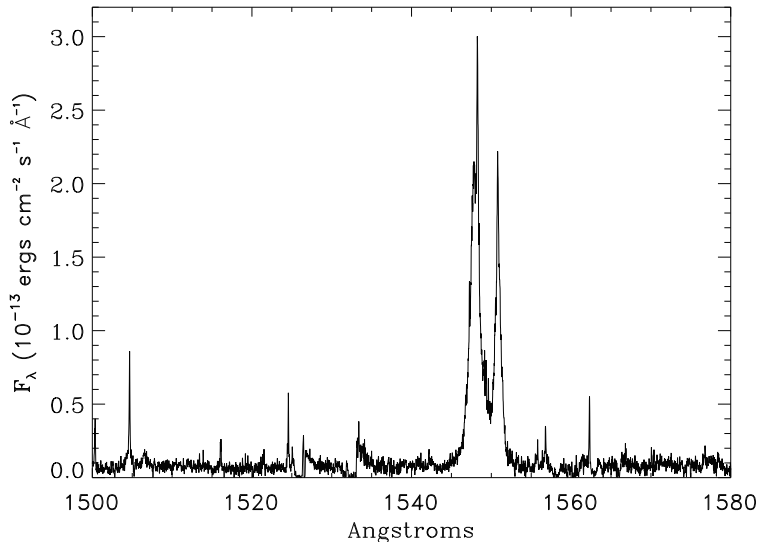


Figure 4. A region near the C IV resonance lines in the Class I source RU Lupi. Three distinct types of emission are visible. The strong lines of C IV are formed in the accretion flow, in 10^5 K gas near the accretion shock. The $\lambda\lambda 1526, 1533$ Å Si II lines are formed in the cool wind, and exhibit blueshifted P Cygni absorption profiles. The narrow emission lines are H₂ Lyman transitions (Ardila et al 2002a), fluorescently pumped by H I Lyman α . The H₂ most likely is circumstellar. This spectrum was obtained with HST/STIS; the aperture subtends a 3×9 AU region centered on the star.

flux, but which are not actively accreting. These objects have near- and far-IR excesses, but lack the UV continua and strong emission lines indicative of accretion. Examples of these objects are V773 Tau and V836 Tau.

Class III The Naked or Weak² T Tauri stars (Walter 1987) are pre-main sequence on the basis of their masses and radii, but they lack evidence of optically thick circumstellar material. They are magnetically active, with X-ray and UV emissions similar to those of young active main sequence stars and active binary systems. Many have dark starspots (see Fig. 5). Examples of Class III objects include V410 Tau, HD 283572 (Walter et al 1987), and Parenago 1724 (Neuhäuser et al 1998).

The decay of the far-UV emission from Class I through Class III is illustrated in Fig 6.

1.2. The Magnetospheric Accretion Model

A cohesive theory of the magnetosphere of the T Tauri stars was developed by Shu et al (1994, 1997). The X-wind model posits a quasi-dipolar magnetic

²or Wimpy

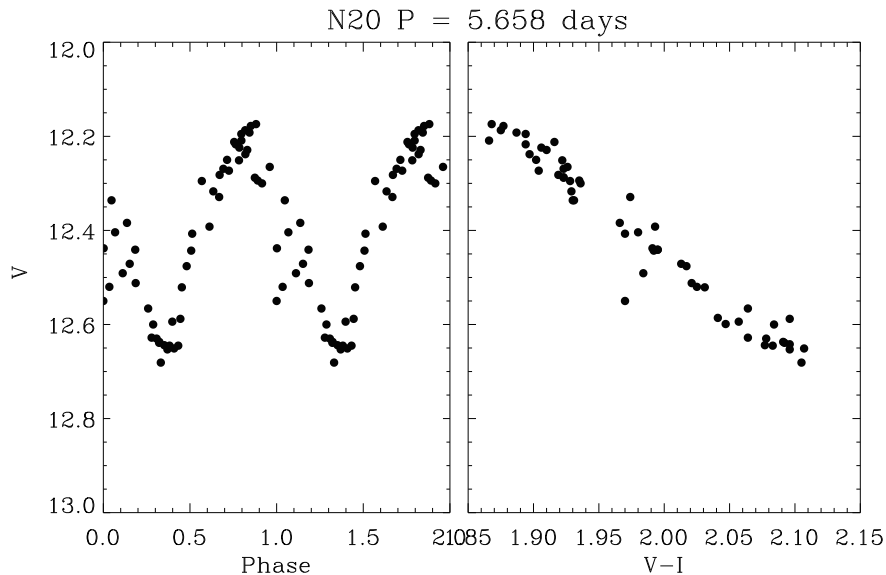


Figure 5. Photometry of the naked T Tauri star LkCa 7 (Herbig et al 1986). Data are from Herbig et al (1986) and Walter et al (1988), supplemented by unpublished observations by C. Ambruster, A. Brown, J. Neff, and F. Vrba, and span the six years from January 1984 through December 1989. A periodogram analysis gives a strongest period of 5.66 days. The left panel shows the folded V-band light curve; the amplitude and period are stable over this interval. The phase is arbitrary. The 0.5 magnitude peak-to-peak amplitude indicates that the spot filling factor is about 50%. The right panel shows that the star gets redder as it gets fainter, as expected for solar-like starspots.

configuration emerging from the stellar photosphere at high latitude and intersecting the partially-ionized circumstellar disk on the midplane. The star is forced to corotate with the disk at the radius where the field threads the disk (disk-locking). This disk-locking is thought to explain the fairly slow rotation rates seen in many Class II stars (Edwards et al 1993). Centrifugal forces constrain the ionized material in the disk to funnel along the magnetic field lines, so that the accretion occurs at high latitudes, and not in an equatorial boundary layer. Winds (and Herbig-Haro flows) emerge at the stellar poles, and perhaps from the surface of the disk. The X-ray emission may arise in compact solar-like loops below this magnetic canopy, or in larger confined structures. The copious UV and optical line emission arises above the accretion shock, near the high latitude footprints of the large scale magnetic field. Such a magnetic topology may also be able to channel the bi-polar flows seen in many Class 0, I, and II objects. Muzerolle et al (2001) have successfully reproduced the cool (H I, Na I) line profiles in accreting systems using a magnetospheric accretion model.

The X-wind model is schematically illustrated in Figure 7. More colorful artist's conceptions of T Tauri stars are presented in Figure 8. The picture on the left is by Mark A. Garlick (<http://space-art.co.uk/>); the figure on the right is from Patrick Hartigan (<http://sparky.rice.edu/~hartigan/research/tts.html>).

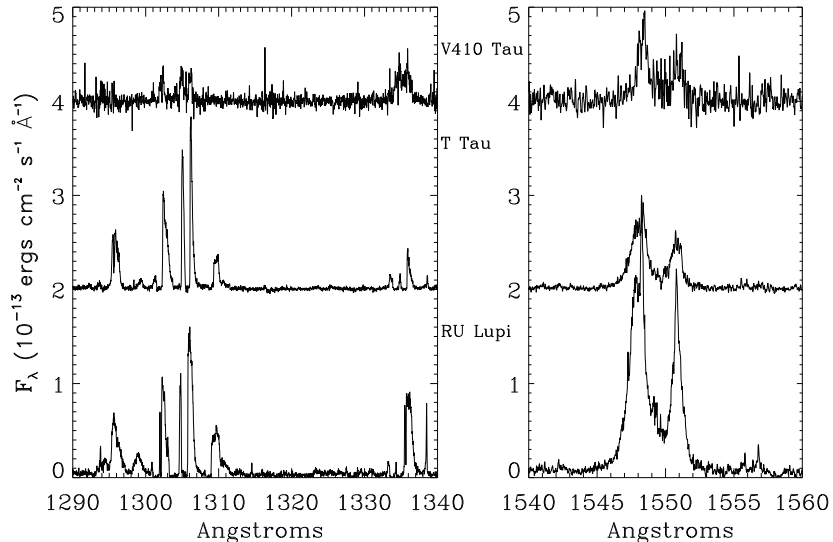


Figure 6. Representative lines from HST/STIS spectra of low mass PMS stars. RU Lupi is Class I; T Tau is Class II; V410 Tau is Class III. Fluxes are offset by 2 units; the flux of V410 Tau is multiplied by a factor of 5. The fluxes of V410 Tau are consistent with those expected from an active star (e.g., AB Dor) at 140 pc. The left panel shows the O I and C II lines, which are formed in the winds in the T Tauri stars, but in the lower chromospheres of active stars. The right panel shows C IV, formed in the accretion stream in the accreting systems and in the transition region of solar-like stars. The narrow spikes atop C IV $\lambda 1548\text{\AA}$ in RU Lupi and T Tau are H_2 lines, as are the lines between 1555 and 1560 \AA .

As you should infer by now, T Tauri stars have it all: magnetic fields, mass infall and mass outflow, coronae and winds, dark spots and bright plages.

Additional (but not unambiguous) evidence for large loops in the PMS stars comes from observations of X-ray flares and of radio emission. Quasi-static loop modelling of flares (e.g., Tsuboi et al 1998; 2000) suggest loop lengths in excess of the stellar radius. However, Favata et al (2001), using hydrodynamical loop models, claim that the same flares can be understood as emission from loops with lengths much less than the stellar radius. In the radio, Phillips et al (1991) showed that the emission from some Class III sources is resolved in VLBI. Although Phillips et al (1996) showed that the ~ 0.3 AU extent of the HD 283447 (V773 Tau) radio source resolved into two point sources at the separation of the binary system, Massi et al (2002) observe periodicities in the radio flux which they interpret as arising from interactions of loops with sizes of order the ~ 0.3 AU semimajor axis of the binary system.

Much as the sculptor facing the proverbial marble block, all we need do to make the Sun out of a T Tauri star is to strip away all that isn't there now.

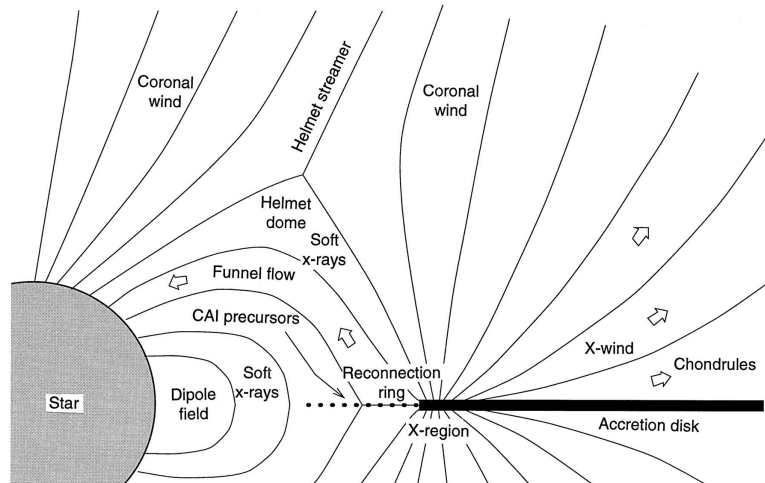


Figure 7. A schematic illustration of the magnetospheric model of classical T Tauri stars, from Shu et al (1997).

1.3. Relevance of the T Tauri Stars to Solar Magnetic Evolution

From the point of view of this exposition, the salient feature of the classical T Tauri stars is the large scale quasi-dipolar magnetic field. There is strong, albeit indirect, evidence for such features, from the disk locking in the Class II sources through the high latitude inflows. The large scale field regulates the disk, but it is generated in the star. There is no reason to expect the large scale field to vanish when the circumstellar disk dissipates. In the following sections I will present evidence that a strong global-scale magnetic topology persists well after the T Tauri phase of stellar evolution.

1.4. Implications for the Earth

The energetics of the T Tauri stars certainly effect the planetary formation process. The ionizing radiation penetrates the disk, mildly ionizing it (Igea & Glassgold 1999). This permits the stellar magnetic field to lock onto the disk, and enforce the disk-braking. By affecting the ionization, the X-ray flux may affect the disk chemistry. In the context of the X-wind model, Shu et al (2001) are able to explain the chondrules, small inclusions in meteorites that appear to have been rapidly melted and then slowly cooled by some violent events early in the history of the Solar System. At a later epoch the ionizing radiation is thought to account for the differential isotopic fractionation of noble gasses observed in the Solar System (Hunten et al 1988; Pepin 1991). Feigelson et al (2001) speculate about the creation of the isotopic anomalies seen in meteorites by proton fluxes from large flares from the pre-main sequence Sun.

But as wild as the young Sun was, all this seems to have little relevance for the evolution of the Earth and its biology, for the simple reason that the Earth as we know it was not yet there. The last major impact, a collision between the proto-Earth and a Mars-sized object that melted the Earth's crust, likely blew off the primordial terrestrial atmosphere, and resulted in the creation of Earth's

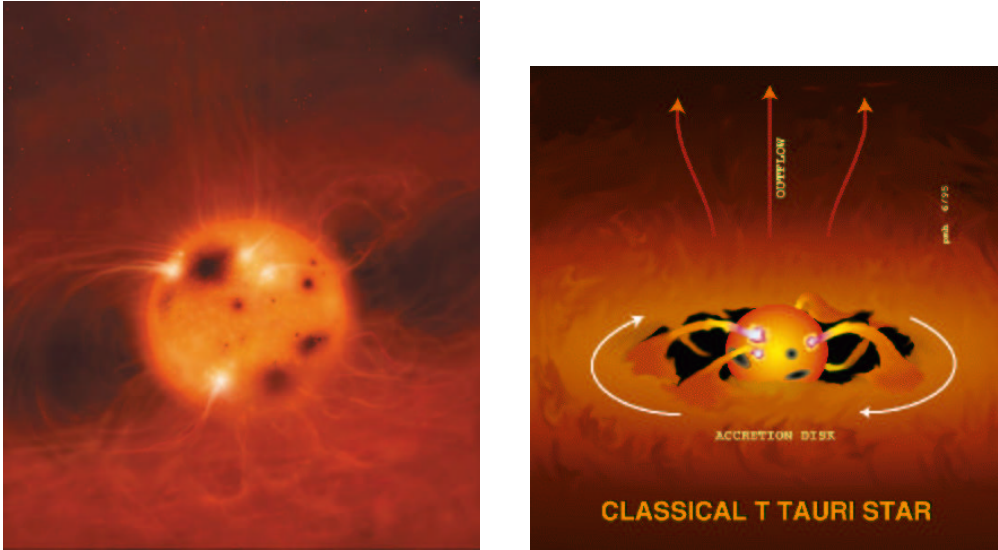


Figure 8. **Left:** A rendition of a T Tauri star by Mark A. Garlick. It appears that we are viewing the star from near the equatorial plane and inside the Keplerian co-rotation radius. The accretion flow is passing over and under us, and is channeled onto the star at high magnetic latitudes. Actively accreting magnetic funnels are lit up; large dark spots exist at high latitude. **Right:** An annotated rendition of a T Tauri star by Patrick Hartigan, showing the inner hole and the magnetic funnels.

Moon, is still nearly 10^8 years off. However, depending on when its last major impact occurred, it is possible that the pre-main sequence Sun had some effect on the early Martian biosphere.

2. Part II. The ZAMS Sun: Paradigm Lost

If one defines the zero-age main sequence (ZAMS) as the point of minimum luminosity on the evolutionary tracks, the Sun reached the ZAMS after about 15 Myr, with a luminosity of $0.43 L_{\odot}$. From the point of view of life on Earth, this is still pretty early in the game. The last major impact - the one between the proto-Earth and the fifth planetary-mass object in the inner Solar System - won't occur for another 80 Myr. This impact would have melted the Earth's surface and blasted away much of the primordial atmosphere. Only after this could Earth's surface cool (a requisite for life as we know it) and its atmosphere stabilize. By this point the Sun had warmed up, and its luminosity had reached $0.75 L_{\odot}$. The equilibrium temperature on Earth was well below the freezing point of water, but presumably greenhouse gasses kept the Earth warm (the well-known faint young Sun paradox).

100 Myr is the age of the Pleiades. G stars in the Pleiades rotate faster than the Sun, but there is no typical period (Soderblom et al 1993): about 20% of the G and K stars are rapid rotators with $v \sin i > 30 \text{ km s}^{-1}$. At younger

ages, such as in the 50 Myr-old α Per cluster, a larger fraction of the solar-mass stars are rapid rotators.

I present in this section a tale of two stars which may be representative of the ZAMS Sun. Both are early K stars, with masses of about $0.8 M_{\odot}$. Both are ultra-rapid rotators: the laws of physics suggest that as a star contracts down its Hayashi track, once the disk dissipates and the disk-locking mechanism becomes inefficient or nonexistent, conservation of angular momentum will cause the star to spin up (Bouvier et al 1997). Unless the Sun's protoplanetary disk lingered for tens of million of years (a distinct possibility since so far, after the discovery of some 100 planetary systems, our Solar System still appears unique), the Sun probably went through a phase as an ultra-rapid rotator. I illustrate the properties of the ultra-rapid rotators with K stars for the simple reason that they are more common than G stars, hence are brighter and better observed.

2.1. AB Dor

AB Doradus (HD 36705; K0-2 IV–V), the brightest ($V=6.7$) of the ultra-rapid rotators ($P_{rot}=0.51479$ d; $v \sin i=91$ km s $^{-1}$), is the quintessential active young single star. AB Dor exhibits large flares (e.g., Robinson & Collier Cameron 1986), large starspots (Anders et al 1992), and large coronal and chromospheric fluxes (e.g., Pakull 1981; Vilhu et al 1991; Schmitt et al 1998; Ake et al 2000).

The parallax (Guirado et al 1997) places the star at 15 pc, slightly above the zero-age main sequence (Collier Cameron & Foing 1997), with a probable age close to that of the Pleiades. AB Dor is the brightest member of a wide multiple star system. The dM4e star Rossiter 137B (AB Dor B) is a common proper motion companion at an angular distance of 10 arcsec (Innis et al 1986; Vilhu et al 1989). Guirado et al (1997) detected a low mass astrometric companion, AB Dor C, with an inferred separation of a few tenths of an arcsec. Guinan & Ribas (2001) suggest that AB Dor C is of substellar mass.

An interesting but no longer unique feature of AB Dor is its transient $H\alpha$ absorptions, attributed to co-rotating material at 2–5 stellar radii (Collier Cameron & Robinson 1989), in the form of cool prominences or $H\alpha$ clouds (Collier Cameron et al 1990). Collier Cameron et al (1999) reported the optical doppler imaging observations from the November 1994 coordinated campaign. As usual, the star featured high latitude dark regions with some low latitude spots; numerous $H\alpha$ prominences, and some flares. Brandt et al (2001) reported on the simultaneous HST/GHRS observations.

The UV observations provide evidence that the $H\alpha$ prominences are not the only extended gas in the system. The Mg II, Si IV (Fig 9), and C IV resonance lines all show broad emission pedestals underlying the narrower chromospheric emission. Brandt et al modeled the broad pedestal as spatially-extended gas co-rotating with the star, and not to microflaring (e.g., Wood et al 1997) or some other unknown broadening mechanism. The pedestals in the Mg II $k&h$ lines are likely to arise in extended prominences (indeed, absorption transients are seen in the Mg II and C IV [Walter 1996a] profiles). By analogy, since their shapes are indistinguishable, the Si IV and C IV pedestals likely have similar origins.

A simple model of gas filling a volume of radius about $3 R_*$, co-rotating with the star, suffices to fit the broad pedestal. This radius is close to the

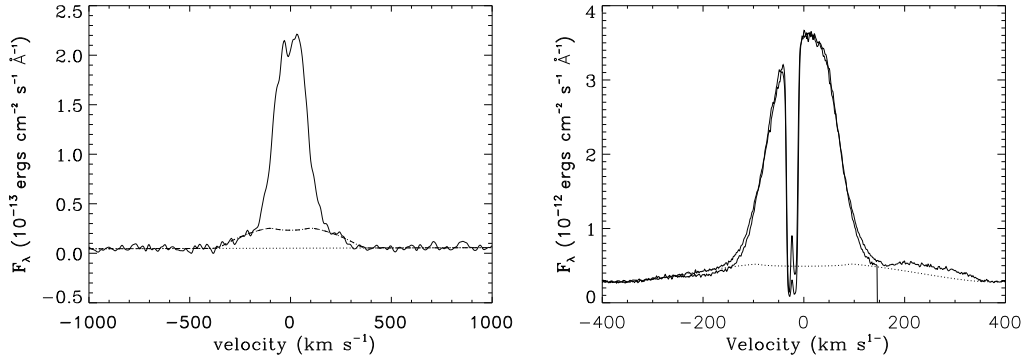


Figure 9. Two quiescent line profiles of AB Dor in November 1994, from Brandt et al (2001), showing the broad emission pedestal underlying the line core. **Left:** The mean Si IV $\lambda 1393$ line profile. The dashed line represents a model for emission from an optically-thin, constant density atmosphere extending out to 3 stellar radii. **Right:** The mean Mg II k (thick line) & h (thin line) profiles plotted on a velocity scale. The h line is scaled by 1.23 and is cut off at $+145 \text{ km s}^{-1}$ by the edge of the detector. The blue wing extends out to about -320 km s^{-1} . The hump on the red wing of the k line (between $+170$ and $+350 \text{ km s}^{-1}$) is the sum of the $\lambda 2797.922$ ($3p \ ^2P_{3/2} - 3d \ ^2D_{3/2}$) and $\lambda 2797.989$ ($3p \ ^2P_{3/2} - 3d \ ^2D_{5/2}$) subordinate lines of Mg II. The dotted line shows the expected emission line profile for an optically-thin uniform density extended atmosphere with a height of 3 stellar radii.

$2.8 R_*$ Keplerian co-rotation radius, and suggests a model wherein the “slingshot prominences” are dense, cooling condensations trapped near the Keplerian co-rotation radius by a magnetic canopy. Collier Cameron & Robinson (1989) argue that centrifugal support provided near the co-rotation radius can make condensations near the tops of large magnetic loops relatively stable. However, van den Oord et al (1998) suggest that the condensations form at lower altitudes and need not be centrifugally supported. If the density of the condensations is comparable to the density of the transition region, the filling factor of the condensations is of order 10^{-5} .

The magnetic topology of AB Dor is far more complex than suggested by the simple X-wind model for T Tauri stars (and the fields of T Tauri stars are likely far more complex too). Much effort has gone into mapping the starspots using doppler imaging techniques (e.g., Unruh et al 1995; Hussain et al 1997; Hussain, this volume), and into mapping the magnetic topology with magnetic doppler imaging (e.g., Jardine et al 1999). Donati et al (1999) find a ring of negative magnetic polarity at high latitude: it is tempting to associate this with the footprints of a global quasi-dipolar field emerging at high latitude, and reconnecting in the unseen hemisphere, but the fields are complex, and the details are beyond the scope of this review. Donati et al (1999) note that there seems to be a non-solar-like component to the field.

The magnetic topology of AB Dor is not unique. The quasi-dipolar large scale field is similar to that postulated for the T Tauri stars. Many other rapid

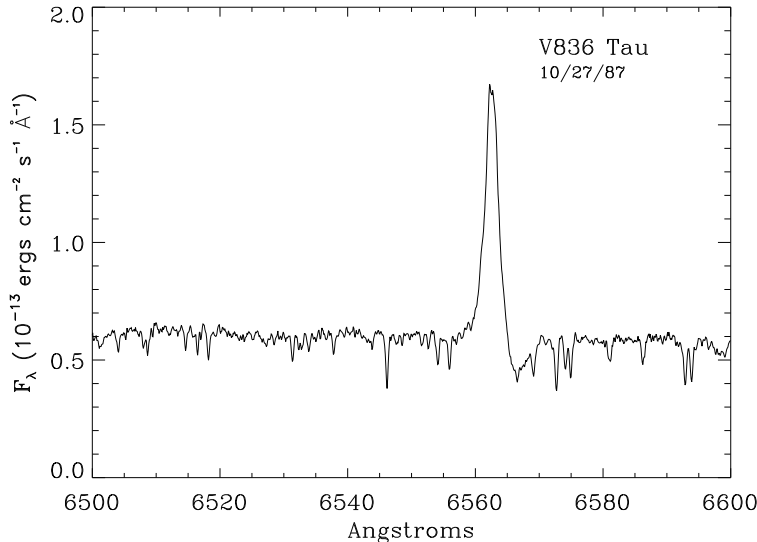


Figure 10. A spectrum of the Class II-III object V836 Tau. The inverse P Cygni line profile is indicative of mass infall; the mean infall velocity is -190 km s^{-1} , with velocities up to -350 km s^{-1} . This star has a small near-IR continuum excess, and the 25 to $100\mu\text{m}$ SED is consistent with an optically thick disk, but the disk is passive, and likely has an inner hole. Despite the lack of steady accretion, sporadic accretion clearly occurs.

rotators are now known to exhibit similar behavior. The PMS star RX J1508.6-4423 shows evidence for extended $\text{H}\alpha$ prominences, but these are seen in emission (Donati et al 2000). This gas is likely trapped at the co-rotation radius by an overlying magnetic canopy. Other stars exhibiting similar behavior include the rapid rotators PZ Tel (Barnes et al 2000), RE 1818+541 (Eibe 1998), HD 197890 (Jeffries 1993; Barnes et al 2001), four G stars in the α Per cluster (Collier Cameron & Woods 1992; Barnes et al 1998), and the dMe star HK Aqr (Byrne et al 1996). All these stars seem to be viewed at fairly low inclinations, which facilitates a view of the condensations in projection against the stellar disk.

Another characteristic sometimes seen in rapid rotators is transient infall, has been reported in BD+22 4409 by Eibe et al (1999). This star is seen at high inclination, so the high latitude prominences would not be expected to occult the stellar disk. Rather, transiently infalling material is seen as a red absorption against the $\text{H}\alpha$ emission profile. In the scenario being put forth here, this infall is material which condenses and flows back to the star along the magnetic field lines anchored at high latitude. Similar transient absorption is seen in PMS stars, such as the Class II-III star V836 Tau (Fig. 10; Wolk & Walter 1996). This star has a passive disk with an inner hole. On this occasion the inverse P Cygni line profile shows evidence for an accretion event. Walter (1999) presents a series of $\text{H}\alpha$ profiles of active stars which show V/R asymmetries and sharp red wings, which can be explained by high latitude accretion.

The similar behavior of the rapidly rotating PMS and ZAMS stars argues for analogous magnetic topologies, and a large scale global magnetic field which survives the T Tauri phase.

2.2. V471 Tau

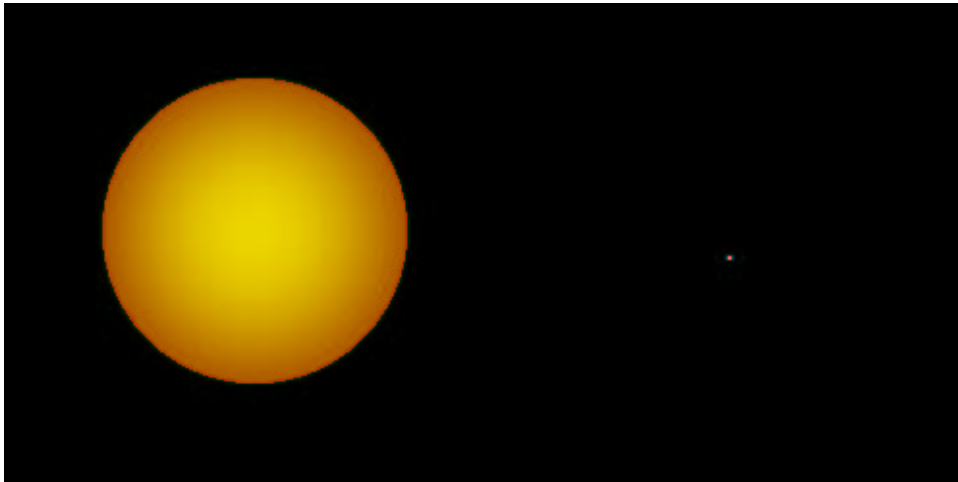


Figure 11. The V471 Tau system at quadrature, drawn to scale. The white dwarf is the dot to the right. The K star radius is $0.95 R_{\odot}$; the white dwarf orbits about 2.5 K star radii above the photosphere of the K star. We make no attempt to draw in the extended atmosphere.

V471 Tau is not a young star. It is a member of the Hyades. However, it rotates in 12.5 hours, much like AB Dor, and acts very much like the young and single ultra-rapid rotators. V471 Tau is an eclipsing post-common-envelope/pre-cataclysmic binary consisting of an active K2 dwarf tidally locked with a hot DA white dwarf (see Figure 11; an animation of the orbit is available here). The orbital period is 12.5 hours; the semi-major axis of the K star is 3.2 K star radii (R_K); the mass ratio is close to unity. It is magnetically active, displaying flares (Beavers et al 1979; Young et al 1983), a photometric wave (Ibanoglu 1978; Skillman & Patterson 1988), coronal X-ray emission (Jensen et al 1986; Wheatley 1998), and emission in the chromospheric lines of Ca II H&K and H α (Skillman & Patterson 1988). Doppler images (Ramseyer et al 1995) reveal a large high-latitude spot. V471 Tau has properties similar to those of the single ultra-rapid rotators and to the rapidly rotating K stars in RS CVn and BY Dra systems. The mass of the K star is assumed to be $0.8 M_{\odot}$. Ramseyer et al (1995) deduce a radius $R_K=0.95 R_{\odot}$ for the K star, which is about 20% greater than normal for a K2 dwarf at the age of the Hyades (see discussion by Ramseyer et al 1995). The K star does not fill its Roche lobe.

This system provides a unique point of view: near eclipse the line of sight to the (approximately point-like) white dwarf passes through the K2V atmosphere. A simple application of Kirchoff's laws shows that where its brightness exceeds that of the K star, the hot white dwarf can be used to probe the atmosphere of the K star (see Fig 12). This is a variant of the technique used to probe the atmospheres of the ζ Aur systems (e.g., Eaton 1993; Bauer & Bennett 2000). In

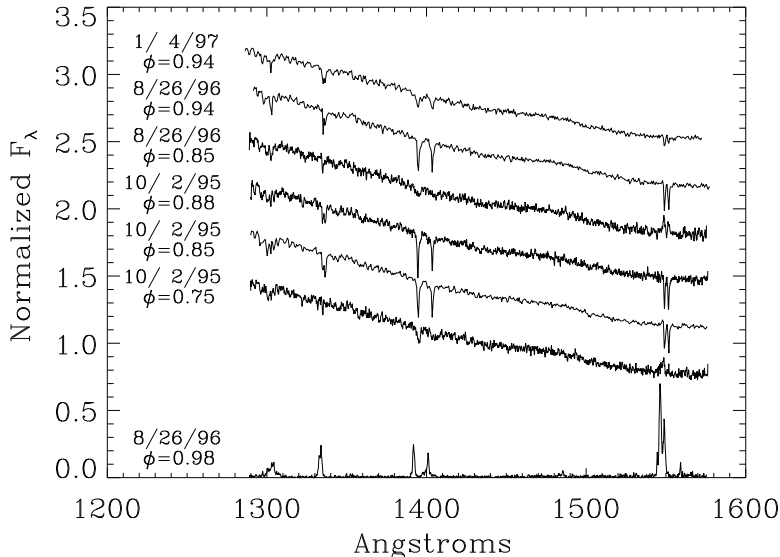


Figure 12. Low resolution spectra of V471 Tau obtained with the HST/GHRS (Kim & Walter 1998; Walter & Kim 2001). At the bottom is a spectrum taken during eclipse showing the K star’s chromosphere. At other phases the continuum of the white dwarf dominates. The out-of-eclipse spectra are scaled by their median flux and offset by 0.35 units. Observations are labeled by date and central phase. The noisier spectra are the short (0.01 orbital cycles) ACCUM-mode observations, smoothed with a Fourier filter. The longer and smoother rapid readout observations sample about 0.045 orbital cycles. The variable strength O I, C II, Si IV, and C IV lines are evident.

this case, we can use the white dwarf to probe the chromosphere and corona in the UV and X-rays.

Guinan et al (1986) first detected absorption lines of C II, C III, C IV, Si II, Si IV, and O I in the white dwarf spectrum between orbital phases 0.88 and 0.12, as the line of sight to the white dwarf passed through the chromosphere of the K star. They interpreted these lines as arising in a chromospheric loop, at temperatures of 10^4 to 10^5 K and electron density n_e of 10^{10} to 10^{11} cm^{-3} , viewed in absorption. The *IUE* spectra offered only a single integrated spectrum; more modern instrumentation affords the possibility of obtaining time-resolved spectroscopy; the time variation of the absorption is a probe of the temperature and density structure along the line of sight.

Our HST observations of V471 Tau confirm Guinan’s discovery. As shown in Fig. 12, these transition region absorption lines are prominent and variable in six low dispersion GHRS spectra between orbital phases 0.75 and 0.95 (prior to ingress to eclipse of the white dwarf). The absorption lines are not seen between phases 0.25 and 0.75, when the white dwarf is in front of the K dwarf, and are not always present between phases 0.75 and 0.25.

We obtained three time-resolved GHRS spectra (see Kim & Walter 1998 for details), one of which is shown in Fig. 13. Movies of this and the other



Figure 13. Time-resolved low resolution spectrum of V471 Tau obtained with the HST/GHRS on 26 August 1996. Orbital phases run from 0.926 at the bottom to 0.971 (after ingress to eclipse) at the top. The time resolution is 10 seconds. The wavelength scale is the same as in Fig 12. From left to right, the prominent absorption lines are O I, C II, Si IV, and C IV. Note the variability of the line flux: the absorption lines disappear on occasion, and saturate at other times.

GHRS observations at 2 second time resolution are available at [ghrs_100295.gif](#), [ghrs_082696.gif](#), and [ghrs_010497.gif](#). All three sets of spectra were taken prior to ingress, and all show the same general type of variability. Timescales of the variability are a few minutes, which correspond to linear distances of 10^4 to 10^5 km (of order 10% of the K star radius). These may be the sizes of discrete structures in the outer atmosphere of the K star. These features are seen at phases between 0.82 and 0.97 in the time-resolved spectra, which corresponds to gas within $2 R_K$ of the photosphere. In the second movie ([ghrs_082696.gif](#)), note how the lines go into emission during eclipse.

More recently, we have obtained time resolved HST/STIS echelle spectra in the far UV (see Walter & Kim 2001 for details). The gross characteristics are similar to those seen at low dispersion: time variable absorption. However, the higher resolution of the echelle lets us be more quantitative about our deductions (see Fig. 14). The lower two panels in Fig. 14 show parts of the echelle order containing the N V doublet; the wavelength scale runs 1235.8 through 1249.4Å. The data are not flat-fielded: the variation of the continuum flux with wavelength is instrumental. Time and orbital phase increase upwards. The lower image spans orbital phases 0.02 through 0.08 ($0.7 R_K$ height); egress occurred at phase 0.03. The middle image covers phases 0.15 through 0.20 (1.8 to $2.4 R_K$). The N V doublet is detected in emission during eclipse, and in absorption after egress. Note that the line is variable in wavelength, profile, and strength. The thin

lines mark the expected velocities of the K2V star (right), the ISM (center), and magnetically confined gas projected against the white dwarf (thick line). Because the K star rotates synchronously with the orbital period, the projected gas velocity and the orbital velocity of the white dwarf are identical. The lines strengthen with height above the photosphere. Similar structure is seen in C IV and Si IV. The upper panel shows the behavior of the C II absorption between phases 0.02 and 0.08. The line is less optically-thick, and shows the blobby structure more readily. Note the strong interstellar C II line at 1334.532Å.

The mean radial velocity of the absorption tracks the expected radial velocity of gas in rigid-body rotation about the K star, with an RMS velocity dispersion of 12 km s⁻¹. This is expected if the gas is confined in magnetic flux tubes. None of the absorption arises from the surface of the white dwarf: the surface of the white dwarf is redshifted by about 50 km s⁻¹ from the co-rotation velocity. As can be seen in Fig. 14, the absorption is blobby, consisting of discrete features which come and go. The velocity of the distinct blobs can be blueshifted by up to 70 km s⁻¹. The characteristic linear size of the discrete blobs is 20,000 km.

Analysis of the lines shows that the atmosphere is very extended, with strong absorption seen at orbital phase 0.22, nearly to quadrature. The atmosphere gets hotter as one goes up: the C II absorption is seen only close to the surface, while N V, the hottest strong line accessible to the HST, continues to increase in strength with height.

Movies of the N V λ 1238Å spectra on 23 March 1998 at 10 second time resolution are available at stis_v2.gif (phases 0.02 to 0.08) and stis_v3.gif (phases 0.15 to 0.20). The first movie (stis_v2) begins in eclipse (the intensity scale resets as the white dwarf appears); the second ends near quadrature. The two are adjacent HST orbits separated by an Earth occultation. The aspect of the stars is shown in the upper left, and the orbital phase is given in the upper right. In both movies the yellow line is a fit to the data consisting of a quadratic continuum plus zero to three Gaussian lines. The data are averages of 50 seconds of data on 10 second centers, but are otherwise unsmoothed. Note how the number of components (or their velocity separation) is largest as the line of sight passes close to the surface of the K star. The overall line strength increases as the line of sight moves up and away from the K star. The N V line is often saturated. The Si IV and C IV lines behave much like N V.

2.3. Characteristics of Other Active Stars

There is abundant evidence that other active stars, from dMe stars to RS CVn and FK Com stars, share many non-solar like characteristics.

Most rapidly rotating active stars exhibit large dark polar spots or polar crowns (e.g., Strassmeier 2001). A set of doppler images of stars ranging from pre-main sequence stars to active dwarfs to RS CVn systems to active giants (see Fig. 15) is maintained by the Astrophysikalisches Institut Potsdam (AIP) Stellar Activity Group. By solar analogy (ironically, the solar analogy may help cast doubt upon the general applicability of the solar analogy), the dark regions are likely to mark the areas of emergence of magnetic flux. This could suggest a general dipolar topology, with the flux emerging near visible pole reconnecting in the polar regions of the hidden hemisphere.

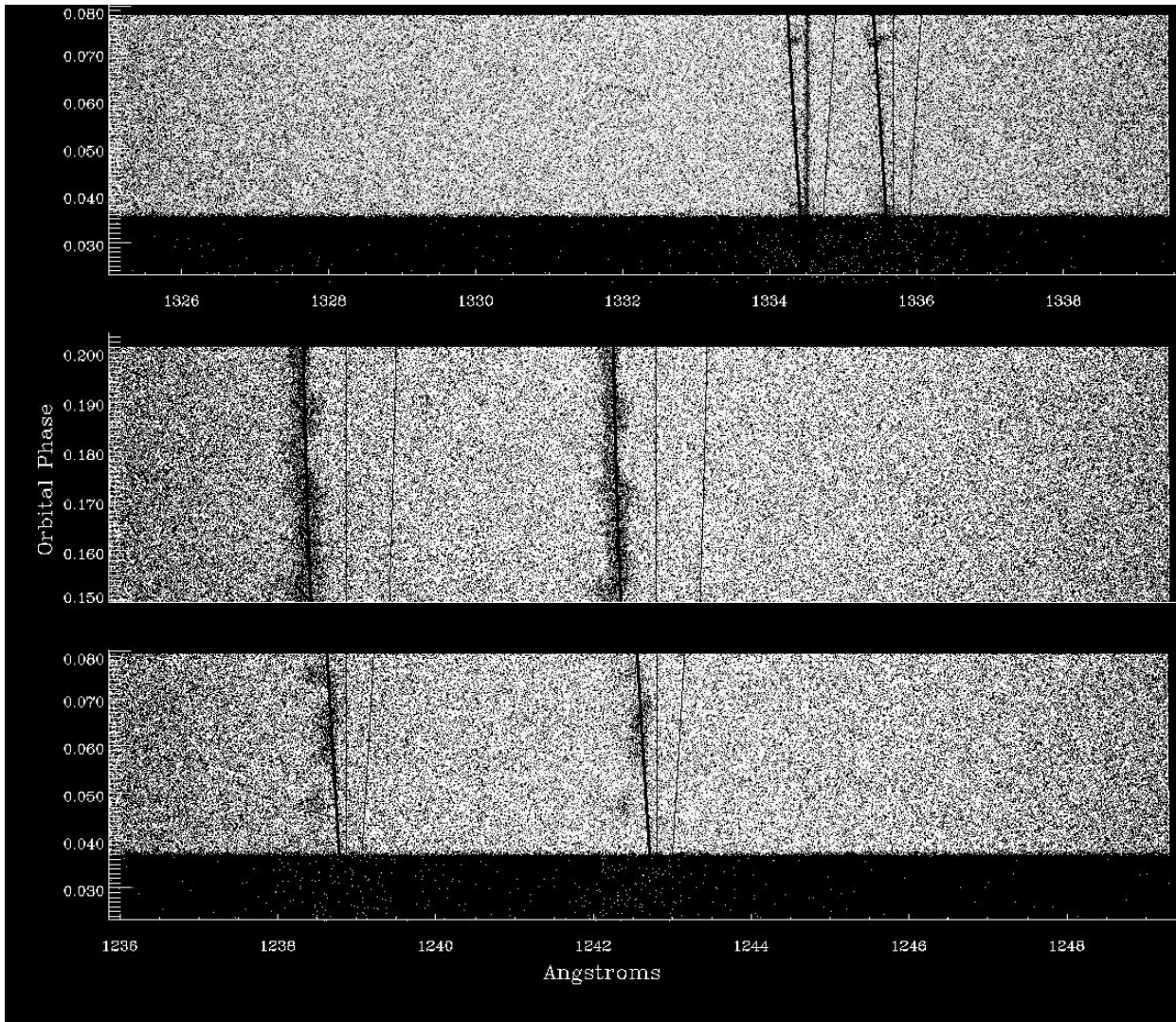


Figure 14. Time-resolved HST/STIS spectra of V471 Tau over two orbits on 23 March 1998. Details are in the text.

The FK Comae stars are particularly interesting from the point of view of stellar activity (although they are not a state the Sun is likely to pass through). These are single rapidly rotating giants. They have prominent photometric waves (starspots; see Fig. 15) and strong coronal (Gondoin, this volume) and chromospheric line emission. FK Comae itself has a prominent polar crown as well as low latitude starspots (Korhonen et al 1999). Olivera & Foing (1999) show that the Hydrogen Balmer emission arises in extended structures, with heights of up to 0.25 stellar radii above the photosphere. The radio and X-ray emission can be modelled jointly as arising in a somewhat extended volume ($\sim 1 R_*$; Hughes & McLean 1987). Scaled to the size of the star, the properties of the FK Comae stars, the ultra-rapid rotators, and the PMS stars are all very similar.

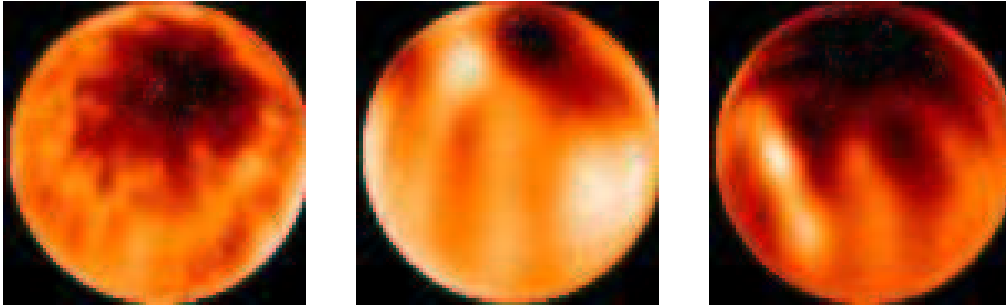


Figure 15. Three doppler images from the AIP Stellar Activity Group web page. On the left is the naked T Tauri star HD 283572 (V987 Tau; spectral type G5); the active G1V ZAMS star EK Dra is centered, and to the right is the G5 giant HD 199178, an FK Comae star. Note the dominant polar spot in all three stars.

In a growing number of cases, there is direct evidence for extended magnetospheres visible at radio wavelengths. RS CVn systems which have been resolved by VLBI observations tend to have magnetospheres with sizes comparable to the Roche lobes (e.g., Beasley & Güdel 2000). The observed sizes, and the circular polarization, require large scale, quasi-dipolar magnetic field configurations with coronal field strengths of order 10 G (e.g., Lestrade et al. 1984; Mutel et al. 1985). These extended radio lobes are not limited to giants: Alef et al (1997) showed that the radio source associated with the eclipsing dMe system YY Gem has an extent of about 2.1 stellar diameters, and Pestalozzi et al (2000) find similarly extended radio emission from the dMe stars YZ CMi and AD Leo.

There is direct evidence for prominence-like structures and other spatially extended gas in a number of RS CVn systems. The 2-day period eclipsing system AR Lac is particularly rich in these phenomena. For example, Neff et al (1989) identified discrete structures in the Mg II h&k line profiles with velocity amplitudes in excess of the photospheric $v \sin i$, suggestive of structures suspended above the surface but in rigid rotation with the photosphere. The pronounced dark hemisphere on the G star in the 1987 Mg II doppler image (Neff et al 1989) is likely due to absorption of the chromospheric Mg II emission by an extended cool cloud or prominence with a size of order $3 R_{\odot}$. While the eclipses of the G star are often sharp, suggesting a true eclipse of compact (solar-like) magnetic structures (e.g., Walter et al 1983), the X-ray light curves show that primary eclipse is often longer than expected for a pure geometric eclipse. The slow egress observed in 1984 (White et al 1990) and the slow ingress observed in 1993 (White et al 1994) are both consistent with absorption by extended structures above the limb of the foreground K star. Walter (1996b) showed that the eclipse of the G star observed by EUVE in 1993 was consistent with a purely geometrical obscuration of the G star, but egress was slow. A simple model requires obscuring material out to $\sim 6 R_{\odot}$, with densities n_e of 10^{11} to 10^{12} cm^{-3} , which is at the upper end of the range observed in solar prominences.

Heuenemorder et al (1989) noted that the $\frac{H\alpha}{H\beta}$ ratio in UX Ari was similar to that in solar prominences, and suggested that low density extended material

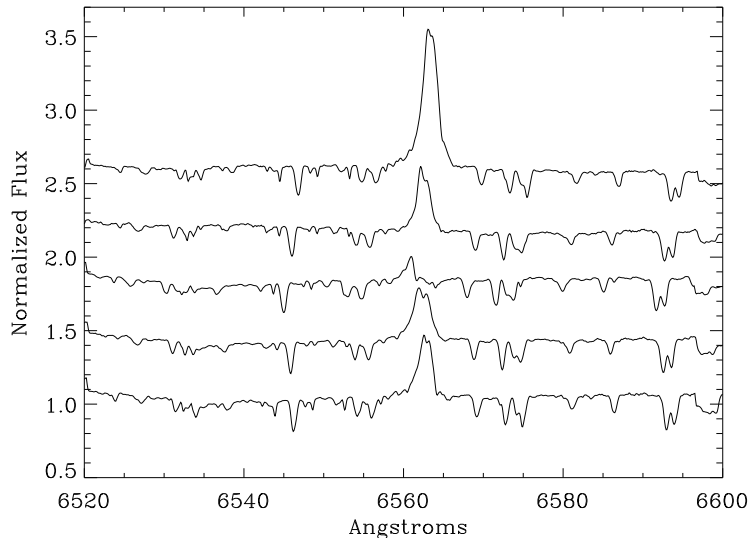


Figure 16. A series of five spectra of the RS CVn system II Peg obtained on 23-27 October 1987 (from bottom up). The continua are scaled to unit median, and subsequent spectra are offset by 0.5 units. The $H\alpha$ profile changes markedly, with most of the variation appearing on the red wing of the line. This can be interpreted as absorption by infalling material, as seen in younger rapid rotators. Note the V/R asymmetry: the blue peak generally exceeds the red peak.

could be the source. Hall & Ramsey (1994) also modeled the $H\alpha$ profiles of 4 RS CVn systems as prominence-like structures with scale heights of order the stellar radius.

$H\alpha$ line profiles of the single-lined RS CVn system II Peg (Fig. 16) show variations which are most simply understood in terms of sporadic infall. Absorption by a co-rotating prominence has a unique spectral signature, crossing the line from blue to red in a time short compared to the rotation period. That the lack of emission is consistently on the red side of the line can be explained by infall. II Peg is observed at a fairly high inclination (about 35° from pole-on); following the arguments of Eibe et al (1999), prominence absorption would be unlikely, but absorption by material draining down the high latitude magnetic flux lines is likely.

The existence of infall begs the question of the source of the infalling material. Unlike the PMS stars, which, even if not actively accreting, almost certainly have a dirty circumstellar environment, the RS CVn systems are well past this stage. A hypothesis is that a global magnetic field which crosses the equator can act as a magnetic canopy, trapping material ejected in flares and coronal mass ejection (CME) events. As this material cools, it may drain back along magnetic lines of force at high latitude.

To summarize, the data strongly suggest that young and active stars, as well as the old and spun-up stars, exhibit evidence for prominent large scale magnetic fields.

3. Part III. The Old Sun: Paradigm Regained?

The large scale quasi-dipolar magnetic topology inferred in active stars appears to be the distinguishing characteristic of the most active stars. Resorting to the solar analogy, the solar-like features arise in a solar-like magnetic field (low lying, small-scale fields), and the non-solar-like characteristics arise in the large scale field component. It is then interesting to speculate that the decay of coronal activity is a consequence of the decay of the global magnetic component.

Güdel et al (1997) have demonstrated that the evolution of the coronae of solar-like stars consists mainly in a rapid fading of a hot (~ 1 keV) component, and a slow decay of a cooler (~ 0.2 keV) component. The Sun has negligible non-flaring emission from a 1 keV component. Young active rapid rotators and active binaries (e.g., Sanz-Forcada, this volume) exhibit close to a 1:1 ratio of emission measures of the hot and cool components. Among the PMS stars (e.g., Skinner & Walter 1998; Favata et al 1998), some 80% of the coronal emission measure arises from the hotter component.

The smooth evolution of the coronal X-rays from the youngest PMS stars through the Sun suggests that the coronal structures responsible for the 0.2 keV plasma are similar on the Sun and stars, while the structures responsible for the 1 keV plasma decay, and are largely absent on the Sun. One can then speculate whether the 1 keV emission is due to a superposition of flares, with the flare rate being large enough in the active stars to yield an apparently quiescent hot component, or whether the hot plasma is associated with longer magnetic loops. In static loop models, the maximum temperature scales as the product of the loop length and pressure $(pL)^{\frac{1}{3}}$ (Rosner et al 1978), so loops with lengths of order the stellar diameter could account for the higher coronal temperatures.

When does a cool star become solar-like? Drake et al (2000) and Orlando et al (2001) show that one can synthesize the observed spectra of low to moderate activity stars by superposition of solar-like structures, at least up to the activity levels of ξ Boo A (G8V; 250 Myr) and ϵ Eri (K2V). Another aspect of solar-like activity is the solar cycle (e.g., Wang 1998). Observations of the chromospheric Ca II K emission cores (e.g., Baliunas et al 1998) show that while the Sun and other low-activity stars tend to show cyclic activity, with periods ranging from about 7 to 15 years, the most active stars generally exhibit only stochastic variability. Over its cycle, the solar X-ray emission measure varies by a factor of 40 in the 0.25-4.0 keV YOHKOH band (Orlando et al 2001), while the mean X-ray luminosities of G stars in young clusters seem to range only over factors of a few at a given rotation rate (in the softer ROSAT band; e.g., Stauffer et al 1994). Repeated X-ray observations of clusters (e.g., Wolk, this volume; Giampapa, this volume) may give some clue as to when magnetic cycles turn on in G stars.

Recent work by Schrijver & Title (2001; see also Schrijver, this volume) shows that one can generate polar crowns from the poleward migration of trailing-polarity magnetic flux in a rapidly rotating star. Their modelling produces polar spots surrounded by concentric rings of alternating polarity field, which may be like the polar rings seen in AB Dor in Zeeman doppler imaging (Donati et al 1999). It is not clear whether these surface field configurations can reproduce the large scale fields inferred in the active stars.

4. Summary

Everything you know is wrong
Firesign Theater -- 1974

The solar analogy fails to explain four types of phenomena persistently seen in very active stars:

- dark high latitude spotted regions - the polar caps or polar crowns.
- the very hot (>10 MK) coronal component.
- the extended radio emission.
- the evidence for infalling material, often at high latitude.

These phenomena can be explained by invoking large scale closed magnetic fields; the transition from active to quiet (solar-like) stars is likewise explicable in terms of the disappearance of these large scale fields.

The evidence strongly suggests that the PMS stars have quasi-dipolar magnetic fields emerging at high latitude, with scale heights of a few stellar radii, based on disk locking, the inner holes, and the accretion line profiles. The persistence of these fields through the naked T Tauri phase, after the dissipation of the circumstellar disk, provides a natural explanation for the dark polar regions, the very hot coronal component, and the infalling material sometimes seen, even in the stars without persistent accretion. At the same time, the resemblance of the cooler coronal component and the transition region line fluxes in the non-accreting stars to those of active solar-like stars argues for the existence of a low lying solar-like corona.

By the time the star reaches the ZAMS its properties depend on its rotation rate. The same non-solar-like phenomena persist among the rapid rotators of this age, suggesting that the large scale magnetic fields also persist. The corona is more solar-like, and the dark spots are now seen at both low and high latitudes. Active rapid rotators, irrespective of age, such as the BY Dra and RS CVn systems, and some dMe stars, also exhibit these phenomena.

The variability of the active stars tends to be stochastic or related to rotational modulation: there is still no compelling evidence for starspot cycles like the 22 year solar magnetic cycle. Aside from flares, the range of variation in a typical active star corona is a factor of a few over timescales of years; the Sun and other inactive stars vary by far more than that. The amplitude of the variation depends strongly on the bandpass used, but can easily exceed a factor of 100 in the hard (1-10Å) X-rays (see Lean 2001 for a review of solar variability).

Today, the Sun has no dominant quasi-dipolar magnetic topology, except in the far-field limit, where the magnetic field is blown around by the solar wind.

So in the end, we have a choice. We can stick with the solar analogy, or we can employ the *T Tauri analogy* to guide our thinking. In the solar analogy, we begin with well-characterized solar-like features, and scale up their densities and volumes to reproduce the observed emission measures. The solar analogy does not explain the high latitude spots, the hot (>10 MK) coronal component, the extended radio lobes, and the persistent evidence for infalling matter in the active stars, because such phenomena do not exist on the Sun. Yet all these phenomena, and more, are evidenced by the T Tauri stars. In the *T Tauri analogy*, we start with everything, and then over time strip away the excesses. The early Sun had large scale quasi-dipolar magnetic structures that facilitated

the non-solar-like phenomena listed above; as that field disappeared so did those phenomena. So which is it to be – the additive solar analogy or the subtractive T Tauri analogy? As recent work (Schrijver, this volume) suggests, the two approaches likely meet in the middle.

Acknowledgments. I thank NASA for its continued support. I also acknowledge some heavy-duty arm twisting on the part of the SOC.

References

- Adams, F.C., Lada, C.J., & Shu, F.H., 1987, *ApJ*, 321, 788
- Ake, T.B., Dupree, A.K., Young, P.R., Linsky, J.L., Malina, R.F., Griffiths, N.W., Siegmund, O.H.W., & Woodgate, B.E. 2000, *ApJ*, 538, L87
- Alef, W., Benz, A.O., & Güdel, M. 1997, *A&A*, 317, 707
- Anders, G.J., Coates, D., & Thompson, K. 1992 *Proc. Astr. Soc. Aus.*, 10, 33
- André, P., Ward-Thompson, D., & Barsony, M. 1993, *ApJ*, 406, 122
- Ardila, D.R., Basri, G., Walter, F.M., Valenti, J.A., & Johns-Krull, C.M., 2002a *ApJ*, 566, 1100
- Ardila, D.R., Basri, G., Walter, F.M., Valenti, J.A., & Johns-Krull, C.M., 2002b *ApJ*, 567, 1013
- Baliunas, S.L., Donahue, R.A., Soon, W., & Henry, G.W. 1998, in *ASP Conf. Ser.* 154, *The Tenth Cambridge Workshop on Cool Stars, Stellar Systems and the Sun*, eds. J.A. Bookbinder & R.A. Donahue (San Francisco: ASP), p. 153
- Baraffe, I., Chabrier, G., Allard, F., & Hauschildt, P.H. 1998, *A&A*, 337, 403
- Barnes, J.R., Collier Cameron, A., Unruh, Y.C., Donati, J.-F., & Hussain, G.A.J. 1998, *MNRAS*, 299, 904
- Barnes, J.R., Collier Cameron, A., James, D.J., & Donati, J.-F. 2000, *MNRAS*, 314, 162
- Barnes, J.R., Collier Cameron, A., James, D.J., & Donati, J.-F. 2001, *MNRAS*, 324, 231
- Bauer, W.H. & Bennett, P.D. 2000, *PASP*, 112, 31
- Beasley, A.J. & Güdel, M. 2000, *ApJ*, 529, 961
- Beavers, W.I., Oesper, D.A., & Pierce, J.N. 1979, *ApJ*, 230, L187
- Bertout, C. 1989, *ARA&A*, 27, 351
- Bouvier, J., Forestini, M., & Allain, S. 1997, *A&A*, 326, 1023
- Brandt, J.C., Heap, S.R., Walter, F.M., et al, 2001, *AJ*, 121, 2173
- Byrne, P.B., Eibe, M.T., & Rolleston, W.R.J. 1996, *A&A*, 311, 651
- Collier Cameron, A., Duncan, D.K., Ehrenfreund, P., Foing, B.H., Kuntz, K.D., Penston, M.V., Robinson, R., & Soderblom, D. 1990, *MNRAS*, 247, 415
- Collier Cameron, A. & Foing, B. 1997, *Observatory*, 117, 218
- Collier Cameron, A. & Robinson R.D. 1989, *MNRAS*, 238, 657
- Collier Cameron, A., Walter, F.M., Vilhu, O., et al, 1999, *MNRAS*, 308, 493
- Collier Cameron, A. & Woods, J.A. 1992, *MNRAS*, 258, 360

- Donati, J.-F., Collier Cameron, A., Hussain, G.A.J., & Semel, M. 1999, MNRAS, 302, 437
- Donati, J.-F., Mengel, M., Carter, B.D., Marsden, S., Collier Cameron, A., & Wichmann, R. 2000, MNRAS, 316, 699
- Drake, J.J., Peres, G., Orlando, S., Laming, J.M., & Maggio, A.J. 2000, ApJ, 545, 1074
- Eaton, J.A. 1993, ApJ, 404, 305
- Edwards, S., Strom, S.E., Hartigan, P., et al, 1993, AJ, 106, 372
- Eibe, M.T. 1998, A&A, 337, 757
- Eibe, M.T., Byrne, P.B., Jeffries, R.D., & Gunn, A.G. 1999, A&A, 341, 527
- Favata, F., Micela, G., & Reale, F. 2001, A&A, 375, 485
- Favata, F., Micela, G., & Sciortino, S. 1998, A&A, 337, 413
- Feigelson, E.D., Garmire, G., Tsuboi, Y., & Pravdo, S. 2001, in *Two Years of Science with Chandra*
- Feigelson, E.D. & Montmerle, T. 1999 ARA&A, 37, 363
- Güdel, M., Guinan, E.F., & Skinner, S.L. 1997, ApJ, 483, 947
- Guinan, E.F., Wacker, S., Baliunas, S., Loesser, J., & Raymond, J. 1986, in *New Insights in Astrophysics: 8 Years of UV Astronomy with IUE*, p. 197
- Guinan, E.F. & Ribas, I. 2001 ApJ, 546, L43
- Guirado, J.C., Reynolds, J.E., Lestrade, J.-F., et al, 1997, ApJ, 490, 835
- Hall, J.C. & Ramsey, L.W. 1994, AJ, 107, 1149
- Hartigan, P., Hartmann, L., Kenyon, S., Hewett, R., & Stauffer, J. 1989, ApJS, 70, 899
- Hartmann, L. 2001, in ASP Conf. Ser. 223, The Eleventh Cambridge Workshop on Cool Stars, Stellar Systems and the Sun, eds. R.J. García López, R. Rebolo, & M.R. Zapatero Osorio (San Francisco: ASP), p. 3
- Herbig, G.H., Vrba, F.J., & Rydgren, A.E., 1986, AJ, 91, 575
- Herbst, W., Holtzman, J.A., & Phelps, B.E. 1982, AJ, 87, 1710
- Heuenemoerder, D.P., Buzasi, D.L., & Ramsey, L.W. 1989, AJ, 98, 1398
- Hughes, V.A. & McLean, B.J. 1987, ApJ, 313, 263
- Hunten, D.M., Pepin, D.O., & Owen, T.C. 1998, in *Meteorites and the Early Solar System*, eds. J.F. Kerridge & M.S. Matthews, (Tucson: University of Arizona) p. 565
- Hussain, G.A.J., Unruh, Y.C., & Collier Cameron, A., 1997, MNRAS, 288, 343
- Ibanoglu, C. 1978, Ap. Space Sci., 57, 219
- Igea, J. & Glassgold, A.E. 1999, ApJ, 518, 848
- Innis, J.L., Thompson, K., & Coates, D.W. 1986, MNRAS, 223, 183
- Jardine, M., Barnes, J.R., Donati, J.-F., & Collier Cameron, A. 1999, MNRAS, 305, L35
- Jeffries, R.D. 1993, MNRAS, 262, 369
- Jensen, K.A., Swank, J.H., Petre, R., et al, 1986, ApJ, 309, L27
- Korhonen H., Berdyugina S.V., Hackman T., Duemmler R., Ilyin I.V., & Tuominen I. 1999, A&A, 346, 101

- Kim, J.-S. & Walter, F.M. 1998, in ASP Conf. Ser. 154, The Tenth Cambridge Workshop on Cool Stars, Stellar Systems and the Sun, eds. J.A. Bookbinder & R.A. Donahue (San Francisco: ASP), p. CD-1431
- Lada, C.J., in *The Physics of Star Formation and Early Stellar Evolution*, eds. C.J. Lada & N.D. Kylafis, (Dordrecht: Kluwer) p. 329
- Lean, J. 2001, in ASP Conf. Ser. 223, The Eleventh Cambridge Workshop on Cool Stars, Stellar Systems and the Sun, eds. R.J. García López, R. Rebolo, & M.R. Zapatero Osorio (San Francisco: ASP), p. 109
- Lestrade, J-F., Mutel, R.L., Phillips, R.B., Webber, J.C., Niell, A.E., & Preston, R.A. 1984, ApJ, 282, L23
- Massi, M., Menten, K., & Neidhöfer, J. 2002, A&A, 382, 152
- Montmerle, T., Grosso, N., Tsuboi, Y. & Koyama, K. 2000, ApJ, 532, 1097
- Mutel, R.L., Lestrade, J-F., Preston, R.A., & Phillips, R.B. 1985, ApJ, 289, 262
- Muzerolle, J., Calvet, N., & Hartmann, L. 2001, ApJ, 550, 944
- Neff, J.E., Walter, F.M., Rodonò, M., & Linsky, J.L. 1989, A&A, 215, 79
- Neuhäuser, R., Wolk, S.J., Torres, G., et al, 1998, A&A, 334, 873
- Oliveira J.M., & Foing B.H. 1991, A&A, 343, 2130
- Orlando, S., Peres, G., & Reale, F. 2001, ApJ, 560, 499
- Pakull, M.W. 1981, A&A, 104, 33
- Pepin, R.O. 1991, Icarus, 92, 2
- Pestalozzi, M.R., Benz, A.O., Conway, J.E., & Güdel, M. 2000, A&A, 353, 569
- Phillips, R.B., Lonsdale, C.J., & Feigelson, E.D., 1991, ApJ, 382, 261
- Phillips, R.B., Lonsdale, C.J. Feigelson, E., & Deeney, B. 1996, AJ, 111, 918
- Ramseyer, T.F., Hatzes, A.P., & Jablonski, F. 1995, AJ, 110, 1364
- Robinson, R.D. & Collier Cameron, A. 1986, Proc. Astr. Soc. Aus., 6, 308
- Rosner, R., Tucker, W.H., & Vaiana, G.S. 1978, ApJ, 220, 643
- Saar, S.H., 2001, in ASP Conf. Ser. 223, The Eleventh Cambridge Workshop on Cool Stars, Stellar Systems and the Sun, eds. R.J. García López, R. Rebolo, & M.R. Zapatero Osorio (San Francisco: ASP), p. CD-292
- Schmitt, J.H.M.M., Cutispoto, G., & Krautter, J. 1988, ApJ, 500, L25
- Schrijver, C.J. & Title, A.M., 2001, ApJ, 551, 1099
- Shu, F., Najita, J., Ostriker, E., Wilkin, F., Ruden, S., & Lizano, S. 1994, ApJ, 429, 781
- Shu, F., Shang, H., Glassgold, A.E., & Lee, T. 1997. Science, 277, 1475
- Shu, F., Shang, H., Gounelle, M., Glassgold, A., & Lee, T. 2001, ApJ, 548, 1029
- Simon, T. 2001, in ASP Conf. Ser. 223, The Eleventh Cambridge Workshop on Cool Stars, Stellar Systems and the Sun, eds. R.J. García López, R. Rebolo, & M.R. Zapatero Osorio (San Francisco: ASP), p. 235
- Simon, T., Vrba, F.J., & Herbst, W. 1990, AJ, 100, 1957
- Skillman, D.R. & Patterson, J. 1988, AJ, 96, 976
- Skinner, S.L. & Walter, F.M. 1998, ApJ, 509, 761
- Soderblom, D.R., Stauffer, J.R., Hudon, J.D. & Jones, B.F. 1993, ApJS, 85, 315

- Stauffer, J.R., Caillault, J.-P., Gagne, M., Prosser, C.F., & Hartmann, L.W. 1994, *ApJS*, 91, 625
- Strassmeier, K.G. 2001, in ASP Conf. Ser. 223, The Eleventh Cambridge Workshop on Cool Stars, Stellar Systems and the Sun, eds. R.J. García López, R. Rebolo, & M.R. Zapatero Osorio (San Francisco: ASP), p. 271
- Tsuboi, Y., Imanishi, K., Koyama, K., Grosso, N., & Montmerle, T., 2000, *ApJ*, 532, 1089
- Tsuboi, Y., Koyama, K., Murakami, H., Hayashi, M., Skinner, S., & Ueno, S. 1998, *ApJ*, 503, 894
- Unruh, Y.C., Collier Cameron, A., & Cutispoto, G., 1995, *MNRAS*, 277, 1145
- van den Oord, G.H.J., Byrne, P.B., & Eibe, M.T. 1998, in ASP Conf. Ser. 150 *New Perspectives on Solar Prominences*, IAU Colloquium 167, eds. D.F. Webb, B. Schmieder, & D.M. Rust, (ASP: San Francisco), p. 251
- Vilhu, O., Ambruster, C., Neff, J.E., Linsky, J.L., Brandenburg, A., Ilyin, L.V., & Shakovskaya, N.I. 1989, *A&A*, 222, 179
- Vilhu, O., Gustafsson, B., & Walter, F.M. 1991, *A&A*, 241, 167
- Walter, F.M. 1987, *PASP*, 99, 31
- Walter, F.M. 1996a, in *Stellar Surface Structure*, IAU Symposium 176, eds. K.G. Strassmeier & J.L. Linsky (Dordrecht: Kluwer) p. 355
- Walter, F.M. 1996b, in *Astrophysics in the Extreme Ultraviolet*, IAU Colloquium 152, ed. S. Bowyer & R.F. Malina (Dordrecht: Kluwer) p. 129
- Walter, F.M. 1999, in ASP Conf. Ser. 158, *Solar and Stellar Activity: Similarities and Differences*, eds. C.J. Butler & J.G. Doyle (ASP: San Francisco), p. 87
- Walter, F.M. & Barry, D.C. 1991, in *The Sun in Time*, eds. C. Sonnett, M.S. Giampapa, & M.S. Matthews (Tucson: University of Arizona) p. 633
- Walter, F.M., Brown, A., Linsky, J.L., et al, 1987, *ApJ*, 314, 297
- Walter, F.M., Brown, A., Mathieu, R., Myers, P., & Vrba, F. 1988, *AJ*, 96, 297
- Walter, F.M., Gibson, D.M., & Basri, G.S. 1983, *ApJ*, 267, 665
- Walter, F.M. & Kim, J.-S. 2001, in ASP Conf. Ser. 223, The Eleventh Cambridge Workshop on Cool Stars, Stellar Systems and the Sun, eds. R.J. García López, R. Rebolo, & M.R. Zapatero Osorio (San Francisco: ASP), p. CD-1073
- Wang, Y.-M. 1998, in ASP Conf. Ser. 154, The Tenth Cambridge Workshop on Cool Stars, Stellar Systems and the Sun, eds. J.A. Bookbinder & R.A. Donahue (San Francisco: ASP), p. 131
- Wheatley, P.J. 1998, *MNRAS*, 297, 1145
- White, N.E., Shafer, R.A., Horne, K., Parmar, A.N., & Culhane, J.L. 1990, *ApJ*, 350, 776
- White, N.E., Arnaud, K., Day, C.S.R., et al, 1994, *PASJ*, 46, L97
- Wolk, S.J. & Walter, F.M., 1996, *AJ*, 111, 2066
- Wood, B.E., Linsky, J.L., & Ayres, T.R. 1997, *ApJ*, 478, 745
- Young, A., Klimke, A., Africano, J.L., Quigley, R., Radick, R.R., & van Buren, D. 1983, *ApJ*, 267, 655